Inhibition of histamine-mediated signaling confers significant protection against severe malaria in mouse models of disease

Walid Beghdadi,[1] Adeline Porcherie,[1] Bradley S. Schneider,[1] David Dubayle,[3] Roger Peronet,[1] Michel Huerre,[2] Takeshi Watanabe,[4] Hiroshi Ohtsu,[5] Jacques Louis,[1] and Salaheddine Mécheri[1]

[1]Unité des Réponses Précoces aux Parasites et Immunopathologie and [2]Unité de Recherche et d'Expertise Histotechnologie et Pathologie, Institut Pasteur, Paris 75015, France
[3]Centre National de la Recherche Scientifique, UMR 8119, Université Paris Descartes, 75270 Paris, Cedex 06, France
[4]Research Center for Allergy and Immunology, RIKEN, Yokohama 230-0045, Japan
[5]Tohoku University School of Engineering, Sendai 980-8579, Japan

From the inoculation of *Plasmodium* sporozoites via *Anopheles* mosquito bites to the development of blood-stage parasites, a hallmark of the host response is an inflammatory reaction characterized by elevated histamine levels in the serum and tissues. Given the proinflammatory and immunosuppressive activities associated with histamine, we postulated that this vasoactive amine participates in malaria pathogenesis. Combined genetic and pharmacologic approaches demonstrated that histamine binding to H1R and H2R but not H3R and H4R increases the susceptibility of mice to infection with *Plasmodium*. To further understand the role of histamine in malaria pathogenesis, we used histidine decarboxylase–deficient (HDC$^{-/-}$) mice, which are free of histamine. HDC$^{-/-}$ mice were highly resistant to severe malaria whether infected by mosquito bites or via injection of infected erythrocytes. HDC$^{-/-}$ mice displayed resistance to two lethal strains: *Plasmodium berghei* (*Pb*) ANKA, which triggers cerebral malaria (CM), and *Pb* NK65, which causes death without neurological symptoms. The resistance of HDC$^{-/-}$ mice to CM was associated with preserved blood–brain barrier integrity, the absence of infected erythrocyte aggregation in the brain vessels, and a lack of sequestration of CD4 and CD8 T cells. We demonstrate that histamine-mediated signaling contributes to malaria pathogenesis. Understanding the basis for these biological effects of histamine during infection may lead to novel therapeutic strategies to alleviate the severity of malaria.

CORRESPONDENCE
Salaheddine Mécheri:
smecheri@pasteur.fr

Abbreviations used: APC, allophycocyanin; BBB. blood–brain barrier; CM, cerebral malaria; HDC, histidine decarboxylase; ICAM-1, intercellular adhesion molecule 1; MC, mast cell; MFI, mean fluorescence intensity; MGG, May-Grünwald Giemsa; mRNA, messenger RNA; *Pb*, *Plasmodium berghei*; TCTP, translationally controlled tumor protein; VCAM-1, vascular cell adhesion molecule 1.

Our previous research demonstrated that the saliva of *Anopheles stephensi* induces a rapid degranulation of cutaneous mast cells (MCs) in mice, followed by an influx of neutrophils at the bite site and lymph node hyperplasia (1). Moreover, this mosquito saliva–induced inflammatory response leads to a down-regulation of subsequent T cell–mediated immune responses, as assessed by a model of the delayed hypersensitivity reaction. This down-regulation of antigen-specific T cell responses is MC dependent (2). These results led us to hypothesize that inflammatory responses influence the course of infection with *Plasmodium* parasites.

Some reports indicate that specific components of the innate immune system, including eosinophils (3), basophils (4), and MCs (5), could play important roles in the pathogenesis of malaria. Increased levels of histamine in plasma and tissue, derived from basophils and MCs, are associated with the severity of disease in humans infected with *P. falciparum* and in several animal models of infection with *Plasmodium* (6–8). In addition, higher levels of IgE, which binds to basophils and MCs and can trigger histamine release, are associated with the severity of infection with *P. falciparum* (9).

The effects of histamine are exerted through three classical G protein–coupled histamine receptor subtypes termed H1R, H2R, and H3R, which are thoroughly described pharmacologically (10), and a recently identified fourth member of the histamine receptor family, H4R (11). H1R mediates most of the proinflammatory

A. Porcherie and B.S. Schneider contributed equally to this work.

effects of histamine (12). The antiinflammatory and immunosuppressive effects of histamine, such as inhibition of polymorphonuclear chemotaxis (13), IL-12 secretion by monocytes, and induction of IL-10 production (14), are largely dependent on stimulation of H2R, which is coupled to the adenylyl cyclase pathway. IL-10, on the other hand, is a suppressor cytokine and a major regulatory agent of inflammatory responses (15). H3R elicits an increase in intracellular calcium concentration and regulates cytokine release in alveolar macrophages and MCs (16). Histamine enhances intracellular Ca^{2+} concentration and actin polymerization in immature DCs via activation of H1R and H3R, which also enhances chemotaxis of these cells. In maturing DCs, histamine promotes an increase of cAMP and IL-10 production, whereas IL-12 secretion is inhibited (17). These histamine-mediated effects on cAMP and IL-10, as well as inhibition of IL-12 secretion, are mainly mediated by H2R and H3R. In addition, histamine inhibits the capacity of mature DCs to induce allogeneic Th1 responses, suggesting that histamine might influence the polarization of Th cell development (17) .

Histamine also modulates several biological functions of vascular endothelial cells. During an acute inflammatory response, the histamine-induced increase of P-selectin (CD62P) expression on endothelial cells mediates the initial capture of inflammatory cells, including neutrophils, from the blood (18). In vascular endothelial cells, H1R stimulation leads to several cellular responses, including the release of nitric oxide (19), and enhancements in vascular permeability, particularly in postcapillary venules as a result of endothelial cell contraction (20, 21). Several of these effects of histamine might be exploited by *Plasmodium* to survive in its mammalian host. The increase in vascular permeability appears to be a component of malaria pathogenesis and could be advantageous for the parasites, as sporozoites or blood-stage parasites, because it facilitates their entry and exit from blood vessels. The vasodilatory effects of histamine might promote the spread of the parasite through the vasculature, and histamine can increase endothelial expression of thrombomodulin, which is both an anticoagulant and a receptor for parasitized erythrocyte sequestration. Finally, the putative benefit of histamine signaling to *Plasmodium* is strongly supported by the existence of a parasite-derived homologue of the mammalian histamine-releasing factor known as translationally controlled tumor protein (TCTP).

The aim of this work was to directly assess the relevance of histamine in malaria pathogenesis and its association with disease severity. Using mice genetically deficient in H1R ($H1R^{-/-}$), H2R ($H2R^{-/-}$), and histidine decarboxylase ($HDC^{-/-}$), as well as targeting the four histamine receptors (H1R, H2R, H3R, and H4R) by antihistamine drugs, we demonstrate a deleterious effect of histamine-associated inflammatory

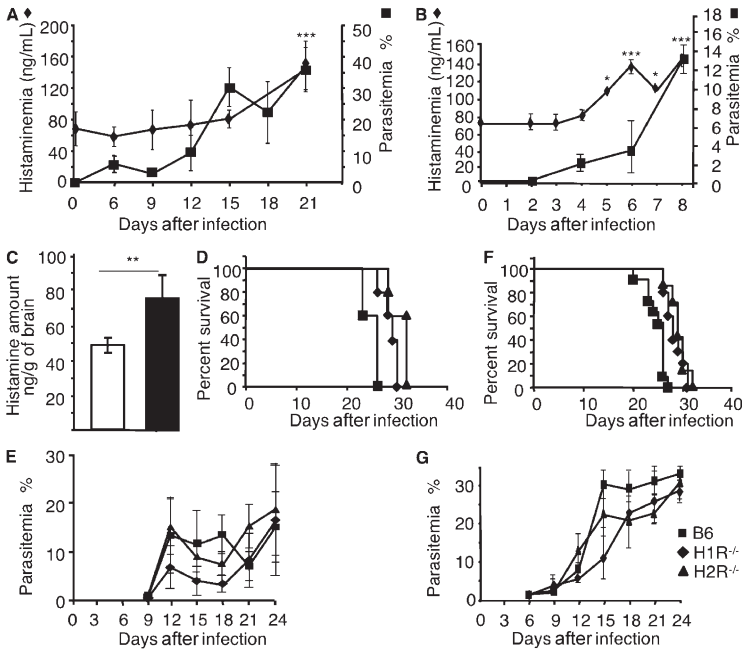

Figure 1. Role of H1R and H2R in *Pb* infection. Histamineamia was measured by ELISA in naive and infected C57BL/6 mice at different time points after inoculation of *Pb* NK65 (A) or *Pb* ANKA (B) through mosquito bites. Values represent the mean ± SD. ***, P = 0.003 (A); * and ***, P < 0.04 and 0.004 (B), respectively, versus plasma histamine levels in uninfected mice. (C) The determination of histamine levels was performed in the brains from naive and infected C57BL/6 mice 7 d after the inoculation of *Pb* ANKA through mosquito bites. Data represent the mean ± SD. **, P < 0.003. Wild-type C57BL/6 mice (squares) or $H1R^{-/-}$ (diamonds) and $H2R^{-/-}$ (triangles) mice were infected either with infectious mosquito bites (seven to nine per mouse; D and E) or with 10^6 infected erythrocytes per mouse (F and G). Survival and parasitemia were recorded. Significant differences were observed between C57BL/6 and $H1R^{-/-}$ and $H2R^{-/-}$ mice after infection by mosquito bites (n = 7; P < 0.042 and 0.035, respectively; D), and after infection with erythrocytes (n = 7; P < 0.008 and 0.007, respectively; F). Differences in parasitemia between groups were not significant. Each group consisted of seven mice. Data shown are from three independent experiments.

responses in malaria infection. Therefore, suppressing the biological effects of histamine may prove to be a new strategy to reduce the severity of diseases resulting from infections with *Plasmodium* parasites.

RESULTS

H1R- and H2R-mediated signaling play a role in the pathogenesis of infection with *Plasmodium berghei* (*Pb*)

In a preliminary attempt to appraise the impact of histamine on the course of infection with *Plasmodium*, we compared histamine levels in the plasma of mice infected or not with *Pb*. As shown in Fig. 1, the levels of histamine in plasma increased significantly over time in C57BL/6 mice inoculated with *Pb* NK65 and *Pb* ANKA by mosquito bites. It can be observed that although histamine levels increased relatively late at day 15 ($P = 0.045$) and became significantly high only at the onset of disease (day 20; $P = 0.003$; see Fig. 2 A) after infection with *Pb* NK65, the rise in histaminemia occurred much earlier and became significantly higher at day 5 after infection ($P < 0.04$) and constantly increased up to the time of death of most of the mice (day 8; $P < 0.004$; see Fig. 3 C) after infection with *Pb* ANKA. A similar increase in histamine levels has been reported in humans infected with *P. falciparum* (22). We also determined the levels of histamine in the brains of infected mice after infection with *Pb* ANKA, which causes cerebral malaria (CM), and found significantly higher amounts of histamine as compared with control mice (Fig. 1 C). To assess whether histamine signaling plays a role in the pathogenesis of malaria, we first determined the mortality and parasitemia of mice genetically deficient for H1R or H2R infected with parasites from a lethal strain of *Pb* NK65 via *An. stephensi* mosquito bites. Results illustrate that, compared with wild-type C57BL/6 mice, $H1R^{-/-}$ and $H2R^{-/-}$ mice displayed a delayed mortality; specifically, death was delayed by 3 d in histamine receptor–deficient mice (Fig. 1 D). Interestingly, comparable parasitemia was observed between mice from the three groups (Fig. 1 E). To determine whether the relative resistance of $H1R^{-/-}$ and $H2R^{-/-}$ mice was confined to the preerythrocytic stage of infection, mice were also inoculated with infected erythrocytes, and mortality and parasitemia were monitored. Although mice from all groups infected in this manner died earlier than when infected through mosquito bites, a similar pattern of divergence between wild-type C57BL/6 mice and $H1R^{-/-}$ and $H2R^{-/-}$ mice was observed (Fig. 1, F and G). These data indicate that regardless of the developmental stage of the parasites used for infection, histamine interaction with either H1R or H2R hasten the fatal outcome, thus suggesting that the detrimental effects of histamine on the course of disease operate during the late stage of infection.

These findings were confirmed using a pharmacological intervention consisting of repeated administration of four histamine inhibitors—levocetirizine (H1R inhibitor), cimetidine (H2R inhibitor), imetit (H3R inhibitor), and JNJ 7777120 (H4R inhibitor)—before infection with 5×10^5 blood-stage parasites (*Pb* NK65). Mice treated with either levocetirizine or cimetidine died significantly later than similarly infected but untreated mice (Fig. 2 A). In contrast, imetit and JNJ 7777120 had no effect on mice survival as compared with untreated mice. Again, there was no difference in the parasitemia between antihistamine-treated or untreated mice when infected with blood-stage parasites (Fig. 2 B).

Susceptibility to infection with *Pb* is associated with the *HDC* gene

Because histamine is known to act through four receptors (H1R, H2R, H3R, and H4R), obstructing signaling of only a single histamine receptor still permits manifestations of the histamine effects by the other receptors. Therefore, to determine the effect of histamine on the course of disease induced by *Plasmodium* in a comprehensive manner, we used mice deficient in HDC, the enzyme that converts histidine into histamine. As a result of this mutation introduced into the

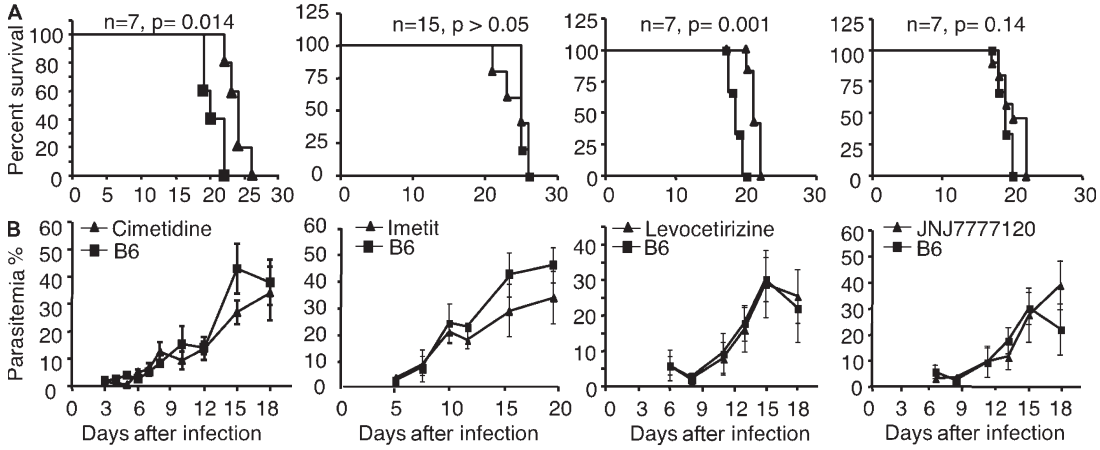

Figure 2. Prolonged survival after treatment with antihistamine drugs. Wild-type C57BL/6 mice were left untreated (squares) or treated (triangles) with the histamine inhibitors levocetirizine, cimetidine, imetit, and JNJ7777123 (for H1R, H2R, H3R, and H4R, respectively) before and during infection with 10^6 infected erythrocytes per mouse. Survival (A) and parasitemia (B) were monitored over time. These data are from three independent experiments. No significant difference was observed for parasitemia between groups (7–15 mice per group). Data are shown as means ± SD.

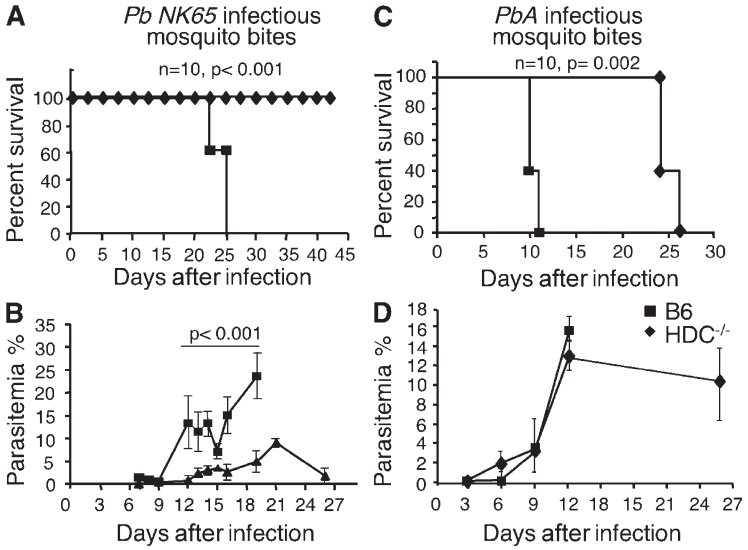

Figure 3. HDC$^{-/-}$ mice are resistant to lethal infection by two *Pb* strains of parasites. Mortality (A and C) and parasitemia (B and D) were recorded for wild-type C57BL/6 mice (squares) or HDC$^{-/-}$ mice (diamonds) infected via mosquito bites with *Pb* NK65 (A and B) or with *Pb* ANKA (C and D). Groups consisted of 10 mice. Differences in parasitemia are significant at each time point from day 12 until day 19 ($P < 0.001$) in B but not in D, and data are shown as means ± SD. Three independent experiments were performed with similar results.

HDC gene, mice cannot produce histamine. HDC$^{-/-}$ mice were infected with *Pb* NK65 via mosquito bites, and mortality and parasitemia were monitored over time. Strikingly, no mortality was observed in HDC$^{-/-}$ mice during the period of observation (>35 d) as compared with wild-type C57BL/6 mice, which died within 25 d after infection (Fig. 3 A). In contrast to C57BL/6 mice, which developed high levels of blood-stage parasites (mean = 12% of RBCs), only 30% of HDC$^{-/-}$ mice developed a blood-stage infection with only low levels of parasitemia (<2% of RBCs) and, ultimately, cleared the parasites (Fig. 3 B).

To examine whether the resistance to disease demonstrated by HDC$^{-/-}$ mice was restricted to one strain of *Pb* and whether histamine signaling affected progression to CM, mice were infected via mosquito bites with *Pb* ANKA parasites, which cause CM, and their survival and parasitemia were monitored. As expected, C57BL/6 mice infected with *Pb* ANKA died from CM within 10 d (Fig. 3 C). All C57BL/6 mice displayed neurological signs within 9–11 d (23), and death occurred within the next 24 h (median survival = day 10). In sharp contrast, HDC$^{-/-}$ mice did not develop CM and died later (median survival = day 24) of parasitemia-induced anemia (Fig. 3 D) without neurological signs (Fig. 3 C). These data strongly suggest that histamine is involved in the pathogenesis of CM, confirming and extending the connection between histamine signaling and malaria disease severity.

The resistance of HDC$^{-/-}$ mice to CM induced by the inoculation of parasites via mosquito bites prompted us to explore at what stage of parasite development histamine mediated this effect; thus, we assessed whether these mice were similarly resistant to infection with blood-stage parasites. After infection with 10^6 infected erythrocytes, C57BL/6 mice were susceptible to CM, displaying characteristic neurological signs before dying within 8 d (median survival = day 7; Fig. 4). In contrast, HDC$^{-/-}$ mice did not exhibit signs of CM, and death occurred on average at day 20, which was consistent with hyperparasitemia-induced anemia (Fig. 4). These data indicate that the resistance of HDC$^{-/-}$ mice to CM does not depend on the stage of parasite development used for infection. These data also suggest that histamine signaling mediates its detrimental effect later in infection, but they do not exclude the possibility that histamine signaling also plays a role at the preerythrocytic stage.

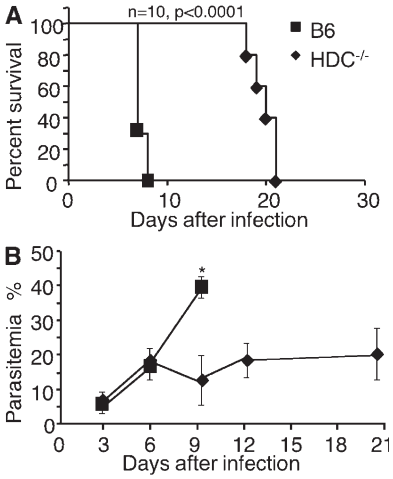

Figure 4. HDC$^{-/-}$ mice are resistant to lethal infection by blood-stage parasites. Survival rates (A) and parasitemia (B) were compared between wild-type C57BL/6 mice (squares) and HDC$^{-/-}$ mice (diamonds) that received 10^6 *Pb* ANKA–infected erythrocytes i.p. per mouse. *, $P < 0.02$ for parasitemia. The cumulative results of four independent experiments (10 mice per group) are shown. Data are shown as means ± SD.

Role of the blood–brain barrier (BBB) during CM

A central feature of CM pathology after infection with *Pb* ANKA is the alteration of the BBB (24). Increased BBB permeability may be mediated through the action of vasoactive amines, such as histamine (25), released from perivascular brain MCs (26, 27). To assess the status of the BBB during infection in our model system, C57BL/6 and HDC$^{-/-}$ mice were infected with 10^6 *Pb* ANKA–parasitized erythrocytes, and the BBB integrity was determined by an Evans blue dye exclusion assay. At day 7, when C57BL/6 mice develop neurological signs, the BBB permeability was evaluated by visualization of the dye extravasation in the brain, as reflected by the appearance of a blue color in the cerebral cortex (Fig. 5 A). In contrast to infected C57BL6 mice, infected HDC$^{-/-}$ mice did not show significant extravasation of the dye in the cerebral cortex, similar to uninfected C57BL/6 and HDC$^{-/-}$ control mice. Thus, infected C57BL/6 mice have a disruption of the BBB integrity concomitant with the appearance of neurological signs, whereas similarly infected HDC$^{-/-}$ mice do not exhibit detectable alteration of their BBB integrity.

The neurological signs that characterize CM are generally accompanied by the sequestration of infected erythrocytes in the cerebral vasculature. Histological analysis of brain sections obtained from naive or infected C57BL/6 mice revealed large erythrocyte aggregates observed in sections from olfactory bulbs and other anatomical parts of the brain (Fig. 5 B, panels 1 and 2). In sharp contrast, such aggregates were not detected in samples from infected HDC$^{-/-}$ mice (Fig. 5 B, panels 5 and 6).

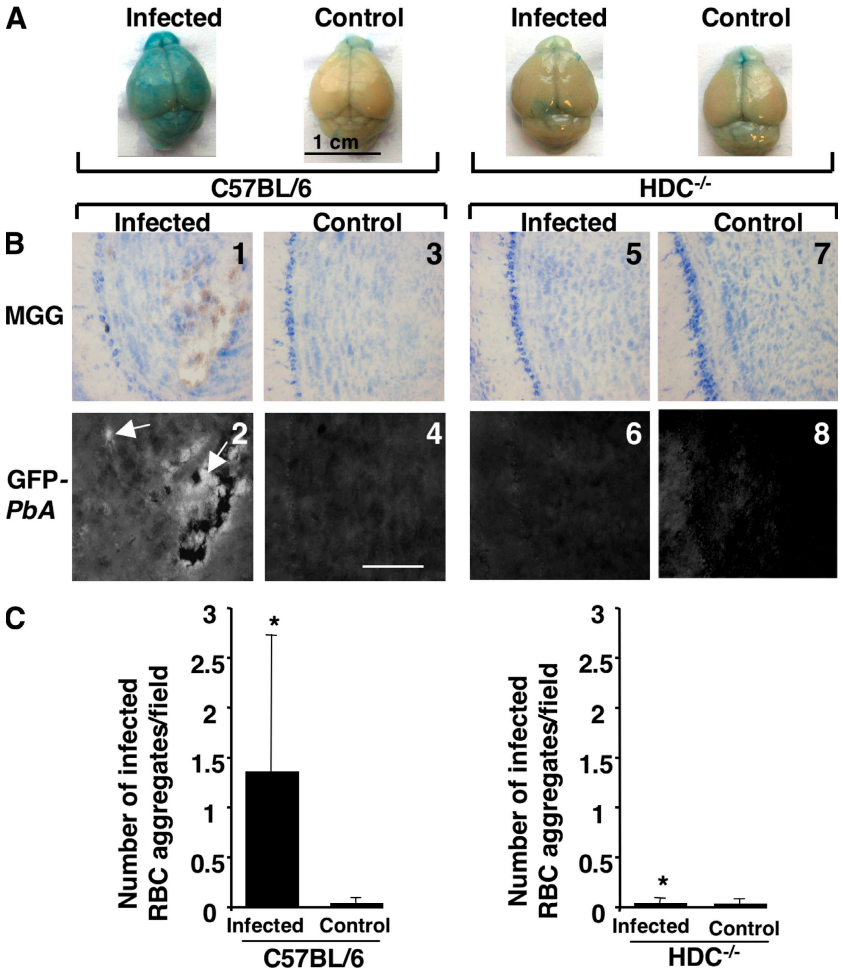

Figure 5. Preserved BBB and a lack of sequestration of infected erythrocytes in the brain of HDC$^{-/-}$ mice. (A) Wild-type C57BL/6 mice and HDC$^{-/-}$ mice were inoculated i.p. with 10^6 infected erythrocytes of *Pb* ANKA per mouse. At day 7 after infection, mice were injected with a solution of Evans blue dye and were perfused with PBS 1 h later, and macroscopic observation was made of the brains. Brains from uninfected mice were used as controls. (B) Sections from the brains of the same mice were stained with MGG. Blood-stage parasites associated with sequestered erythrocytes (panels 1 and 2) in the brain could be visualized by fluorescence because of their expression of GFP (white, arrows; panel 2). No fluorescence could be observed in brain sections from uninfected and infected HDC$^{-/-}$ mice (panels 5 and 6). Data shown are representative of six mice per group. (C) The density of erythrocyte aggregates in brain sections of infected and control HDC$^{-/-}$ and C57BL/6 mice were expressed as the mean of aggregates per field and counted in 50 consecutive microscopic fields. These data are from two different experiments. *, $P < 0.05$ between infected HDC$^{-/-}$ and C57BL/6 mice. Data are shown as means ± SD. Bar, 100 μm.

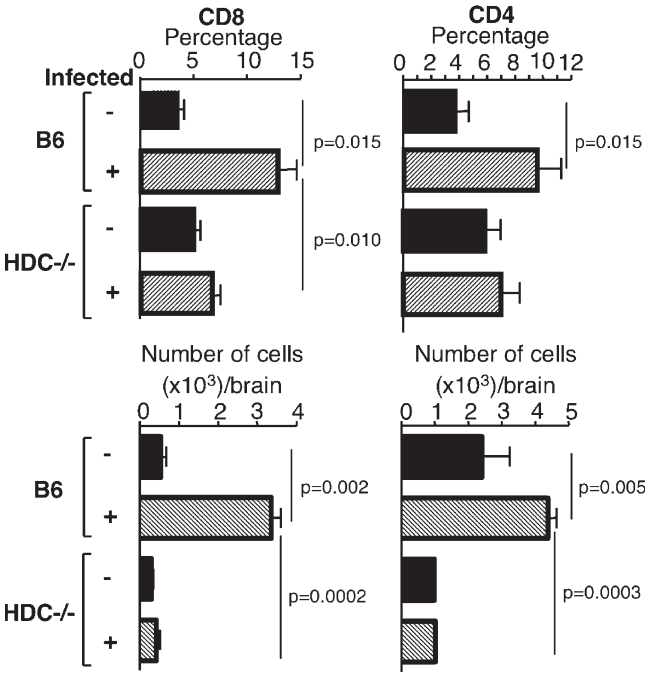

Figure 6. Absence of sequestration of CD4⁺ and CD8⁺ T cells in the brains of infected HDC$^{-/-}$ mice. At the coma stage (day 7 after infection), brains from C57BL/6 and HDC$^{-/-}$ mice infected with 10^6 infected erythrocytes of *Pb* ANKA per mouse were taken, and leukocytes associated with cerebral tissue were analyzed for the presence of CD4⁺ and CD8⁺ T cells and expressed as a percentage of the total cell population and as absolute numbers per brain. Six mice per group were used. Values represent the means ± SD from three experiments.

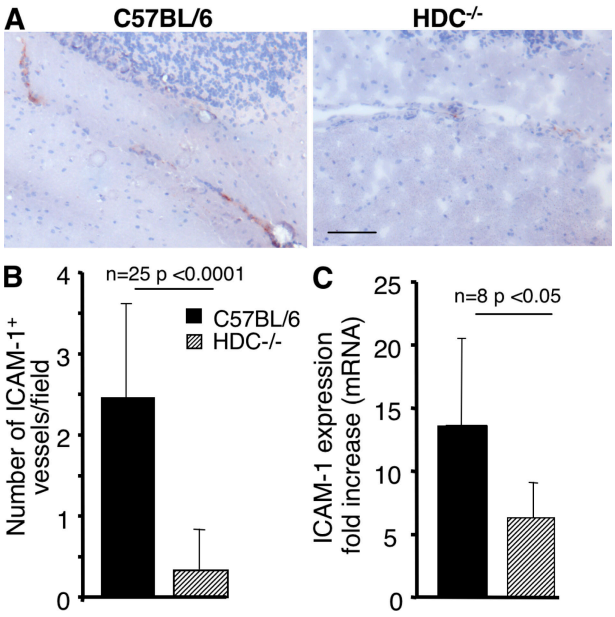

Figure 7. ICAM-1 expression in brain vessels of infected C57BL/6 and HDC$^{-/-}$ mice. (A) Histological section showing ICAM-1 expression indicated by immunohistochemical staining, using anti–ICAM-1 mAb, of brain sections from infected HDC$^{-/-}$ and C57BL/6 mice. Photographs from control noninfected mice (not depicted) show <0.5 positive vessels per field in both mice. (B) The number of ICAM-1–positive vessels per field in *Pb* ANKA–infected C57BL/6 and HDC$^{-/-}$ mice. No significant labeling could be detected in naive mice in both mouse strains (<0.5 positive vessels per field). The proportion of ICAM-1–positive vessels was counted from 10 biopsies for each sample, and three mice were used in each group. (C) Comparison of ICAM-1 mRNA transcripts between infected C57BL/6 and HDC$^{-/-}$ mice as measured by quantitative RT-PCR. The relative mRNA levels of ICAM-1 were measured using real-time RT-PCR in brains. The expression levels were normalized to the endogenous control gene GAPDH, and the relative expression levels were calculated using the uninfected animals as calibrators. Data are presented as the means ± SD from two independent experiments. Bar, 100 μm.

Notably, these aggregates consisted mainly of infected erythrocytes, as shown by fluorescence measurable because GFP-expressing parasites were used for infection (Fig. 5 B, panel 2). Quantification of brain lesions, expressed as the number of erythrocyte aggregates in 50 consecutive microscopic fields, confirmed a significantly larger number of infected erythrocyte aggregates observed in C57BL/6 mice as compared with HDC$^{-/-}$ mice (Fig. 5 C). These data show that the maintenance of the BBB integrity in infected HDC$^{-/-}$ mice is associated with a lack of infected erythrocyte sequestration in brain capillaries and an absence of CM.

The resistance of HDC$^{-/-}$ mice to the development of CM after infection with *Pb* ANKA correlates with a drastic reduction of brain-infiltrating T cells and decreased expression of adhesion molecules

During infection with *Pb* ANKA, the development of CM is strongly associated with the recruitment and activation of T cells in the brain (28, 29). Accordingly, we examined whether such T cell recruitment occurred in HDC$^{-/-}$ mice. Brain-infiltrating leukocytes were isolated from C57BL/6 or HDC$^{-/-}$ mice 7 d after infection with *Pb* ANKA, and the percentage and absolute numbers of CD4⁺ and CD8⁺ T cells were determined. Compared with uninfected control mice, infected C57BL/6 mice displayed a 3.6-fold increase in the number of CD8⁺ T cells sequestered in the brain, whereas HDC$^{-/-}$ mice show only a 1.3-fold increase (Fig. 6). Regarding the CD4⁺ T cell sequestration, infected C57BL/6 mice displayed a 2.7-fold increase, whereas HDC$^{-/-}$ mice had only a 1.18-fold increase.

Vascular cell adhesion molecule 1 (VCAM-1; CD106) and intercellular adhesion molecule 1 (ICAM-1; CD54) expression by capillary endothelial cells in the brain tissue mediates the firm and irreversible adhesion of leukocytes through very late antigen 4 (CD49d), lymphocyte function-associated antigen 1 (CD11a/CD18), and Mac-1 (CD11b/CD18), respectively (30, 31). Because ICAM-1 was found in many studies to be associated with CM, we focused our analysis on the expression of this adhesion molecule. We found that ICAM-1 protein was significantly increased in the brain microvessels of CM-susceptible C57BL/6 mice compared with those of CM-resistant HDC$^{-/-}$ mice (Fig. 7 A). To quantify these histological changes, the number of cerebral vessels expressing ICAM-1 was determined by immunohistochemistry.

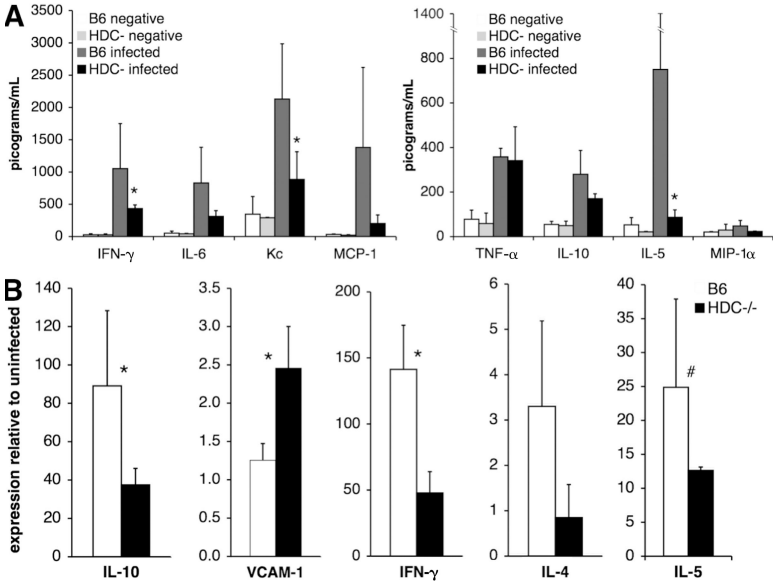

Figure 8. Differential expression of immune signaling genes in C57BL/6 and HDC$^{-/-}$ mice infected with *Pb* ANKA. (A) Serum levels of specific immune and inflammatory proteins were quantified at day 5 after infection by LINCOplex protein assay, and proteins with the highest variation between groups are displayed. (B) Transcription of cytokines and chemokines in the brain ($n > 6$ per group) 7 d after infection as evaluated by real-time RT-PCR. Gene mRNA expression is normalized relative to uninfected controls for each mouse strain, and control mRNA levels did not differ significantly between groups. Data are shown as means ± SD. *, $P < 0.05$; #, $P = 0.05$.

Significantly fewer ICAM-1–positive vessels per field (Fig. 7 B) were observed in infected HDC$^{-/-}$ mice, which are refractory to CM development. Inasmuch as ICAM-1 expression is known to be modulated by histamine (32, 33), we also determined the ICAM-1 messenger RNA (mRNA) expression in the brains of infected mice and found that it was 2.2 times higher in the brains of C57BL/6 mice than in HDC$^{-/-}$ mice ($P < 0.05$; Fig. 7 C). Unexpectedly, VCAM-1 mRNA expression was slightly elevated in HDC$^{-/-}$ brain samples (see Fig. 8 B). These results could suggest that the lower level of CD4$^+$ and CD8$^+$ T cells sequestered within the brain capillaries of infected HDC$^{-/-}$ mice could be at the basis of the failure of these mice to develop CM. Furthermore, the near absence of T cell sequestration in the brain of CM-resistant HDC$^{-/-}$ mice correlates with the low ICAM-1 expression by brain endothelial cells.

Differential production of immunoregulatory and effector molecules between C57BL/6 and HDC$^{-/-}$ mice infected with *Pb* ANKA

The possibility exists that the resistance of HDC$^{-/-}$ mice to CM resulted from an impaired or improved capacity of these mice to produce some immune mediators in response to infection with *Pb* ANKA. Therefore, the levels of expression of various relevant molecules at the mRNA and protein levels were compared between HDC$^{-/-}$ and C57BL/6 mice infected with *Pb* ANKA.

First, serum samples at 5 d after infection with *Pb* ANKA were analyzed by the LINCOplex protein array (Fig. 8 A) to evaluate differences in the expression of some relevant proteins between C57BL/6 and HDC$^{-/-}$ mice. Of the proteins quantified, the most striking differences were observed in inflammation-associated proteins. Serum IL-5 levels in infected C57BL/6 mice were 10-fold higher than infected HDC$^{-/-}$ mice ($P < 0.05$). Similarly, IFN-γ and keratinocyte-derived chemokine were, respectively, two- and threefold higher in infected C57BL/6 mice ($P < 0.05$). Although not statistically significant, IL-6 and monocyte chemotactic protein 1 were markedly reduced in infected HDC$^{-/-}$ mice as compared with infected C57BL/6 mice.

Second, the expression of mRNA specific for immune mediators was quantified. Real-time RT-PCR was used to evaluate cytokines of particular interest in the brains of mice infected for 7 d. IL-10, IFN-γ, and IL-4 expressions were 2.4, 3, and 3 times higher, respectively, in infected C57BL/6 mice than in HDC$^{-/-}$ mice (Fig. 8 B). In support of the serum protein data, IL-5 mRNA levels in the brain were consistently lower in HDC$^{-/-}$ mice (Fig. 8), and treatment of C57BL/6 mice with levocetirizine reduced cerebral IL-5 levels to those seen in HDC$^{-/-}$ mice (not depicted). Collectively, these results exemplify a divergence between C57BL/6 and HDC$^{-/-}$ mice in the expression of several cytokines. Further work is clearly required to determine whether or not these differences are at the basis of the resistance of HDC$^{-/-}$ mice to CM.

The antigen-induced response of specific CD8$^+$ and CD4$^+$ T cells is similarly affected by infection with *Pb* ANKA in C57BL/6 and HDC$^{-/-}$ mice

Differences in the magnitude of the CD4 and CD8 responses to infection between C57BL/6 and HDC$^{-/-}$ mice could result

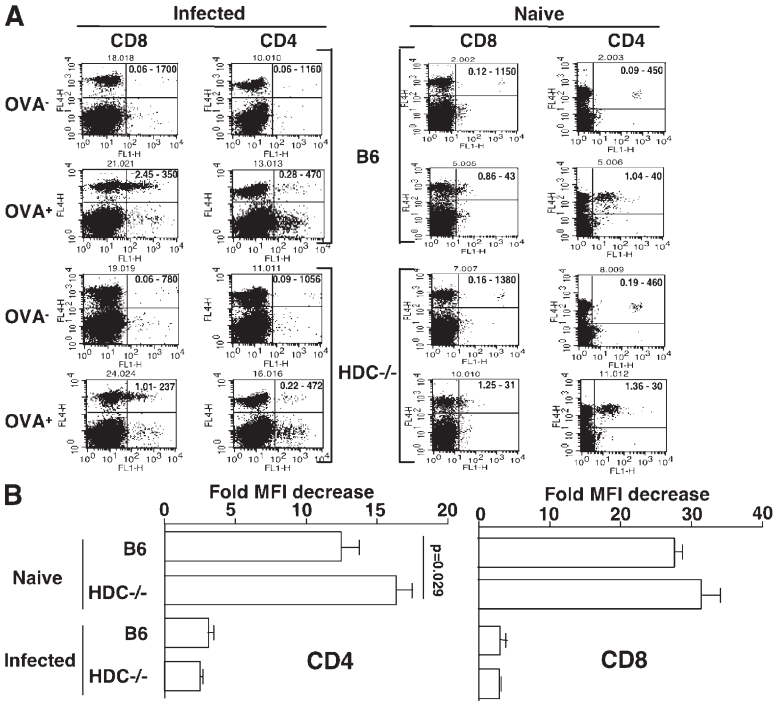

Figure 9. Similar expansion of OT-1 and OT-2 cells in infected C57BL/6 and HDC$^{-/-}$ mice. Wild-type C57BL/6 and HDC$^{-/-}$ mice were infected i.p. with 10^6 infected erythrocytes of *Pb* ANKA per mouse, and 3 d later they received 5×10^6 CFSE-labeled OT-1 or OT-2 cells, followed by injection or not of 1 mg OVA 1 h later. At day 6 after infection, spleen cells were harvested and stained either with APC–anti-CD8 or APC–anti-CD4 mAb, and quadrant FACS analysis was performed (A). Numbers in the top right quadrants indicate the fraction of CFSE/CD8 or CFSE/CD4 double-positive cells and the MFI, respectively. The proliferative response of OT-1 and OT-2 cells was expressed as a ratio between the MFI of CFSE-labeled cells from mice that received OVA to the MFI of those that did not (B). These data were obtained using three mice per group, and the experiment was replicated twice. Values are expressed as the means ± SD.

in dissimilar manifestations of CM between mice from these two strains. Therefore, in an attempt to assess whether infection with *Plasmodium* interferes differently with the development of T cell responses in C57BL/6 and HDC$^{-/-}$ mice, the proliferative capacity of OVA-specific CD4 and CD8 cells in response to specific stimulation was examined in the syngeneic environment of either infected C57BL/6 or HDC$^{-/-}$ mice. 3 d after infection with *Pb* ANKA, C57BL/6 and HDC$^{-/-}$ mice were injected with either CD8 OT-1 or CD4 OT-2 cells labeled with CFSE and treated or not with OVA. The proliferation of these OVA-specific T cells, as reflected by a decrease in the mean fluorescence intensity (MFI) of CFSE-labeled cells, was determined by FACS analysis 3 d later and expressed as the ratio between the MFI of CFSE-labeled cells recovered from mice receiving OVA to the MFI of similarly labeled cells recovered from mice not injected with OVA. Fig. 9 A shows a FACS quadrant analysis of representative samples in which the numbers of CD4$^+$ or CD8$^+$ T cells were plotted against CFSE levels. This was quantitatively analyzed in Fig. 9 B, where no significant difference in the proliferative response of CD8 OT-1 cells could be observed between infected C57BL/6 and HDC$^{-/-}$ mice (a 3 ± 0.09– and 2.9 ± 0.1–fold decrease in MFI, respectively). Similarly, there was no difference in the proliferative response of CD4 OT-2 cells between mice from both strains (a 3.1 ± 0.2– and 2.52 ± 0.01–fold decrease in MFI, respectively). In contrast, in noninfected mice from both strains, CD8 OT-1 cells and CD4 OT-2 cells exhibited a much higher proliferative response (a 27.7 ± 0.06– and 31.5 ± 0.9–fold decrease in MFI for C57BL/6 and HDC$^{-/-}$ mice, respectively, for CD8$^+$ T cells; and a 12.4 ± 0.09– and 16.4 ± 0.07–fold decrease in MFI for C57BL/6 and HDC$^{-/-}$ mice, respectively, for CD4$^+$ T cells). These data indicate that the specific responses of CD4$^+$ and CD8$^+$ T cells are equally affected by infection with *Plasmodium* in mice from both strains and, thus, render unlikely the possibility that differences in T cell expansion between mice from the two strains account for the observed dissimilarity in the susceptibility to develop CM.

The resistance of HDC$^{-/-}$ mice to CM is not affected by depletion of CD4$^+$ and CD8$^+$ T cells

It is well established that CD4$^+$ and CD8$^+$ T cells contribute to CM pathogenesis in wild-type C57BL/6 and CBA mice, in view of the fact that mice depleted of CD4$^+$ and CD8$^+$ T cells fail to develop CM (23–25). Furthermore, our results have shown that the resistance of HDC$^{-/-}$ mice to CM corresponds to a lack of sequestration of T cells in brain capillaries (Fig. 6). Nevertheless, we also decided to assess the possibility that peculiar T cell responses triggered within the distinct environment of HDC$^{-/-}$ mice might account for the inability

of these mice to develop CM. Such T cells could, for example, interfere with the triggering of effector T cell responses mediating CM pathologies in wild-type C57BL/6 mice. Thus, to establish whether distinct parasite-induced $CD4^+$ and $CD8^+$ T cells interfere with the development of CM in infected $HDC^{-/-}$ mice, we studied the course of disease in mice depleted of either of these subpopulations of T cells. As expected, depletion of both $CD4^+$ and $CD8^+$ T cells (Fig. 10 A) completely abrogated the development of CM and improved the survival rate in C57BL/6 mice, which then died from anemia (median survival = 7, 21, and 37 d for mice that were untreated, treated with anti-CD8, or treated with anti-CD4, respectively). Depletion of either $CD8^+$ or $CD4^+$ T cells did not allow CM to manifest in $HDC^{-/-}$ mice (Fig. 10 B). However, CD4 T cell depletion resulted in significantly enhanced survival of infected $HDC^{-/-}$ mice (median survival = 20 and 34 d for untreated and anti-CD4–treated mice, respectively; Fig. 10 B). These data do not clearly support a role for CD8 and CD4 T cells in the resistance of $HDC^{-/-}$ mice to CM, but they draw attention to a possible involvement of $CD4^+$ T cells in malaria pathologies other than CM in $HDC^{-/-}$ and C57BL/6 mice.

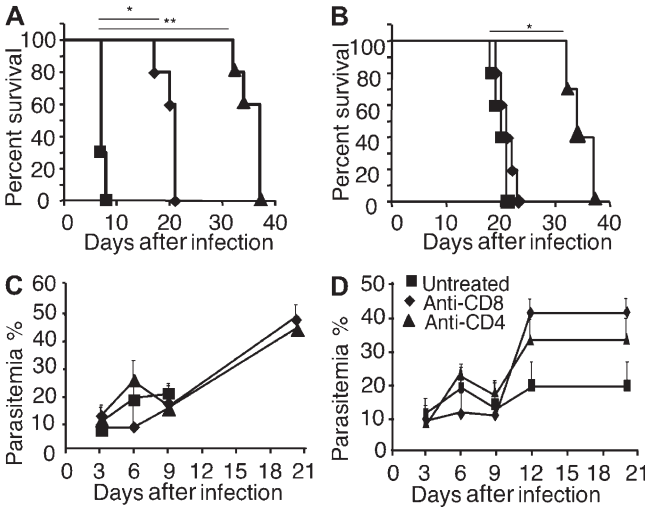

Figure 10. In vivo depletion of CD4 or CD8 T cells did not alter resistance of $HDC^{-/-}$ mice to lethal infection by *Pb* ANKA. Wild-type C57BL/6 (A and C) and $HDC^{-/-}$ (B and D) mice were left untreated (squares) or treated with neutralizing anti-CD4 (triangles) or anti-CD8 mAb (diamonds) before and during infection with 10^6 *Pb* ANKA–infected erythrocytes per mouse. Survival rates (A and B) and parasitemia (C and D) were recorded over time. Six mice per group were used, and data are shown as means ± SD. This experiment was replicated twice. Significant differences in A were observed between untreated and anti-CD8–treated (*, $P < 0.001$) and anti-CD4–treated (**, $P < 0.0001$) mice. A significant difference in B was observed only with anti-CD4–treated mice (*, $P = 0.034$).

DISCUSSION

Histamine is recognized as a key factor in the pathogenesis of allergic diseases. Levocetirizine, a selective H1 antihistamine, controls seasonal allergic rhinitis symptoms in children (34). Use of sedating H1R blockers was also associated with a decreased risk of developing multiple sclerosis (35) and improved the quality of life of patients with chronic idiopathic urticaria (36), suggesting a possible beneficial effect of antihistamines on the onset of some autoimmune diseases. Increased histamine in plasma and tissues is associated with disease severity in human infections with *P. falciparum* and in animal models of malaria (6–8, 22).

Apart from the correlation with immunopathogenesis in other diseases, little is known of the role of histamine in malaria. In this study, we analyzed the influence of histamine on the course of disease in mice infected with *Pb* from two different strains that induce distinct pathologies. This work evaluated the hypothesis that the histamine signaling during infection with *Plasmodium* results in an inflammatory process that exacerbates disease by inducing immunopathology or facilitating the dissemination, adherence, and sequestration of parasites in tissues. Based on divergent approaches using $H1R^{-/-}$ and $H2R^{-/-}$ mice, antihistamine drugs, and histamine-deficient mice, we demonstrate that histamine signaling is associated with the severity of disease.

The mechanisms by which histamine contributes to disease severity and at which stage of the parasite life cycle they operate is unclear. Mice genetically deficient in H1R and H2R, as well as mice treated with H1 and H2 antihistamines, have delayed mortality as compared with similarly infected wild-type mice untreated with the antihistamines, suggesting that the production and binding of histamine to these two receptors are deleterious to the host. However, antagonizing the effects of histamine by interference only at the levels of H1R and H2R had a significant but limited effect with regard to the increase in the mean survival time, possibly because the other factors or histamine receptors, H3R and H4R, also play a role. This is unlikely, however, because imetit and JNJ7777120, H3 and H4 antihistamines known to target H3R and H4R, neither influenced parasitemia nor survival. Thioperamide, a nonselective H3/H4R inhibitor, was also tested and showed no protective effect (unpublished data). To unequivocally determine the effect of histamine on the course of infection with *Plasmodium*, histamine-free mice were used. $HDC^{-/-}$ mice infected with *Pb* NK65 through mosquito bites were highly resistant to malaria disease (90–100% survival up to 35 d after infection), with only 30% of the mice developing blood-stage parasites, which were ultimately cleared. These data strongly suggest that the absence of histamine either resulted in the generation of efficient effector responses against the preerythrocytic and blood stages of the parasite or limited the immunopathology associated with the disease. To expand these results to CM, $HDC^{-/-}$ mice were infected with parasites from *Pb* ANKA. Although $HDC^{-/-}$ mice eventually succumbed from the infection with this strain of *Pb*, they died at much later times than similarly infected control C57BL/6 mice and did not exhibit any signs of CM. These data implicate histamine in the progression to CM, demonstrate that the enhanced resistance of histamine-free mice is not restricted to parasites from a particular strain, and suggest that histamine signaling could lead to enhanced

immunopathological responses. Importantly, results showing comparable parasitemia between groups infected with parasites from *Pb* ANKA do not support the possibility that the inability of histamine-free mice to develop CM resulted from a reduced parasite burden.

In an attempt to better determine at which stage of parasite development histamine mediates its adverse effects, $HDC^{-/-}$ mice were also infected with *Pb* ANKA–parasitized RBCs, thus bypassing the preerythrocytic phase. Identical to what was observed after infectious mosquito bites, histamine-free mice did not develop CM and survived significantly longer than similarly infected control C57BL/6 mice. These data indicate that although histamine is produced during all stages of infection with *Plasmodium* parasites (i.e., by histamine-producing MCs in the skin and in the liver during the preerythrocytic stage of parasites development, and by histamine-producing basophils in the blood where infected RBCs circulate), the pathogenic effects of histamine are likely prevailing in the latter stages of infection. However, the possibility that histamine also plays a role in the skin and/or the liver during the initial phases of the infection cannot be excluded. Indeed, during the initial phases of the infection, specifically the preerythrocytic stages of parasite development, histamine release may be triggered in the dermis when sporozoites are inoculated via mosquito bites. In this context, *Anopheles* saliva induces MC degranulation (1). During later phases of infection, particularly during the blood stage of parasite development, histamine production can be elicited from circulating basophils either via the cross-linking of parasite-specific IgE antibodies or by TCTP, a parasite-derived homologue of the histamine-releasing factor. TCTP has been found in the plasma of patients infected with *P. falciparum* and was shown to trigger histamine release from basophils and IL-8 secretion from eosinophils (37). The existence of a *Plasmodium* protein that stimulates histamine release lends support to the hypothesis that histamine signaling is advantageous to the pathogen and, thus, harmful to the host. These findings could provide a rational basis for higher levels of histamine in blood and in tissues during malaria as a result of the activity of vector- or parasite-derived constituents. Our results (Fig. 1) clearly revealed a progressive increase in histaminemia during the course of infection in C57BL/6 mice. Amplifying the host inflammatory response via histamine signaling may be a strategy developed by the parasites to create conditions advantageous for their own survival and persistence. Although the parasites from the two strains used in our study are lethal for mice, the disease courses that they elicit are quite different. Our results in $HDC^{-/-}$ mice show that in the absence of histamine, the disease severity induced by both parasites was significantly attenuated. The adverse effect of histamine is highlighted by the survival induced after infection with *Pb* NK65 and a delayed non-CM death from *Pb* ANKA resulting from the interruption of histamine signaling. The reason that infection with *Pb* ANKA remains lethal in histamine-free $HDC^{-/-}$ mice is unclear. It seems plausible that even though inhibiting histamine signaling may abrogate immunopathology, it cannot stop the adverse effects of hyperparasitemia. In addition to its distinctive efficiency in producing CM in mice, the possibility exists that *Pb* ANKA also elicits inflammatory mediators, other than histamine, that promote the progression of infection even in $HDC^{-/-}$ mice. Indeed, analysis of several inflammatory proteins and other immune response–associated molecules, including IFN-γ, IL-6, IL-10, keratinocyte-derived chemokine (KC), monocyte chemotactic protein 1 (MCP-1), macrophage inflammatory protein 1α (MIP-1α), cytotoxic T lymphocyte–associated protein 4, and inducible co-stimulator (Fig. 8; and not depicted), indicates that an inflammatory response, although attenuated, was induced in $HDC^{-/-}$ mice. Several studies indicate that the CM pathologies seen in mice after infection with *Pb* ANKA result from the induced proinflammatory immune response. In agreement, IFN-γ, which was shown to be implicated in the pathogenesis of experimental CM (38), reached significantly higher levels in the brain tissue and plasma of CM-sensitive C57BL/6 mice than in $HDC^{-/-}$ mice (Fig. 8, A and B). Similarly, our results showing higher levels of IL-6 in the plasma and increased expression of IL-6 transcripts in the brain of CM-sensitive C57BL/6 than in $HDC^{-/-}$ mice are also in agreement with studies showing higher production of IL-6 in response to TNF-α by endothelial cells of brain capillaries of mice genetically sensitive to CM development (39). Our results, which diverge from murine CM experiments that suggest a protective effect for IL-10 in CM (40) but are in accordance with observations in humans that showed an increase in IL-10 with CM as compared with mild malaria patients (41), show a lower cerebral expression of IL-10 by $HDC^{-/-}$ mice. IL-4 expression corresponds with CM in our model, in agreement with previous studies that demonstrate that deficiency in IL-4 or IL-4Rα leads to higher resistance to *Pb* ANKA (42).

Analogous to the present data that reveal the adverse effects of histamine for the host during infection with *Plasmodium*, a human study demonstrated that the concentration of histamine in plasma was increased by almost fivefold in children suffering from malaria (22). Additionally, in this study, higher levels of histamine were observed in the brains of children with severe malaria as compared to lesser disease presentations. Among the histamine-associated biological activities relevant to features predictive of severe CM in humans are increased intracerebral blood flow (43), increased vascular and BBB permeability (44), and edema (45). Strikingly, the resistance of histamine-deficient mice to CM was clearly identified by a preserved BBB integrity, in contrast to the greatly increased permeability of the brain vasculature with large clusters of infected erythrocytes observed in infected C57BL/6 mice.

In the absence of histamine signaling, profound alterations of the immune response may also occur. A characteristic feature of CM is the sequestration of $CD8^+$ and $CD4^+$ T cells in the brain capillaries (46–48). This was confirmed by results in this study showing a 3.7- and 2.7-fold increase of $CD8^+$ and $CD4^+$ T cells, respectively, in the brain of C57BL/6 mice infected with *Pb* ANKA. Such sequestration in the brain was not observed in similarly infected $HDC^{-/-}$ mice (Fig. 6).

These data suggest that the histamine produced after infection with *Pb* ANKA triggers inflammation that leads to the sequestration of T cells in brain capillaries, a prominent component of CM pathogenesis. In this context, it has been reported that histamine is essential for the recruitment of antigen-specific $CD4^+$ and $CD8^+$ T cells into the site of antigen delivery and the subsequent generation of inflammatory responses (12).

Several studies reported a crucial role of ICAM-1 in malaria pathogenesis, and notably, ICAM-1–deficient mice are protected from CM (49). In this model, ICAM-$1^{-/-}$ mice survived >15 d despite a similar level of parasitemia in wild-type and knockout mice, a phenotype that is comparable to $HDC^{-/-}$ mice. Results from our study confirmed the correlation between ICAM-1 expression, both at the protein and transcript levels, and susceptibility to CM. The low levels of ICAM-1 expression in brain microvascular endothelial cells in histamine-deficient $HDC^{-/-}$ mice (Fig. 8) could represent a mechanism leading to the lack of T cell sequestration in the brain capillaries of these mice. It is interesting to note that ICAM-$1^{-/-}$ and $HDC^{-/-}$ mice, which express similar phenotypes, have in common a reduced synthesis of ICAM-1 molecules, suggesting a control mechanism exerted by histamine on ICAM-1 expression. Indeed, histamine has been shown to stimulate endothelial cells to express ICAM-1 and VCAM-1 (32), and cetirizine, a H1R antagonist, has recently been shown to have antiinflammatory properties through the inhibition of leukocyte recruitment and activation, and by the reduction of ICAM-1 expression on keratinocytes (50) and on conjunctival and nasal epithelial cells (33). Interestingly, a reduction in ICAM-1 and VCAM-1 expression was observed in the brain tissue of infected C57BL/6 mice treated with levocetirizine (unpublished data). In one study, VCAM-1 was identified by microarray analysis as a candidate gene that discriminates between CM-resistant and -sensitive mice in a *Pb* model of CM (51). Our data do not support the assertion that elevated VCAM-1 corresponds to CM, as we observed slightly higher VCAM-1 mRNA levels in $HDC^{-/-}$ mice ($P < 0.05$) as compared with C57BL/6 mice, suggesting an uncertain or, perhaps, protective role for this adhesion molecule in our model. In accordance with our observation of a predominant role for ICAM-1 as compared with VCAM-1 in malaria pathogenesis, infusion of anti–ICAM-1 but not anti–VCAM-1 mAb prevents cytoadherence of infected erythrocytes in a *P. yoelii* model of CM (52).

A possible dissimilarity in the magnitude and quality of the CD4 and CD8 responses elicited by infection with *Pb* ANKA in C56BL/6 and $HDC^{-/-}$ mice could account for the lack of CM in $HDC^{-/-}$ mice. Such differences in the magnitude of the T cell responses could be the result of a divergent ability to suppress antigen-specific T cell responses in C57BL/6 and $HDC^{-/-}$ mice.

Our results showing a similar effect of infection with *Plasmodium* on the specific proliferative response of OT-1 and OT-2 cells in C57BL/6 and $HDC^{-/-}$ mice suggest that the magnitude of T cell responses is similarly affected in C57BL/6 and $HDC^{-/-}$ mice. The effect of infection on the magnitude of the *Pb*-specific T cell response is currently being compared between C57BL/6 and $HDC^{-/-}$ mice. Our results are consistent with previous findings showing that during an acute blood-stage malaria infection T cell responses to *Plasmodium* parasites and other bystander antigens are inhibited (53). Thus, the mechanism by which $HDC^{-/-}$ mice resist CM does not appear to stem from a *Pb* ANKA–induced modification of the peripheral T cell responses, though one could argue that the absence of HDC expression may alter histamine-mediated inflammatory responses that are necessary for the manifestation of some effector functions exerted by $CD4^+$ and $CD8^+$ T cell responses.

To demonstrate directly and unequivocally the implication of histamine in the pathogenesis of CM, attempts were made to revert the CM-resistant phenotype ($HDC^{-/-}$) by frequent injections of histamine into *Pb* ANKA–infected mice. Such treatment failed to induce significant alterations in mortality (unpublished data). This method of repleting mice may, however, not be sufficient because of the low bioavailability and the lability of histamine (54). Nevertheless, our results with antihistamines and genetic knockouts strongly suggest that antihistamine could have a therapeutic value in the treatment of malaria infection, particularly by reducing the likelihood of adverse complications. This is supported by the fact that antihistaminic drugs such as chlorpheniramine potentiate the anti-*Plasmodium* effect of mefloquine, quinine, or pyronaridine (55). It should be pointed out that the antihistamine drugs do not very likely exert their effect directly on the parasite. We performed an experiment in which infected erythrocytes treated with the H1R blocker levocetirizine were compared with untreated infected erythrocytes for their capacity to infect mice. No significant difference regarding survival or parasitemia was observed between the two groups of mice, suggesting that H1 antihistamine drugs exert no direct effect on the parasite (unpublished data).

The present work represents the first comprehensive study documenting the role of histamine in the development of severe pathologies during infection with *Plasmodium*. Although malaria vaccine development remains a central and ultimate goal, alternative chemotherapy-based approaches such as histamine receptor antagonists have the potential to be highly valuable. Such treatment could be part of an integrated control strategy and could also be a useful candidate in intermittent preventive treatment strategies that target specific high-risk groups, such as children and pregnant women. Furthermore, given the availability of antihistamines, such treatment could be implemented rapidly to alleviate the burden of malaria in endemic areas.

MATERIALS AND METHODS

Animals. 6–8-wk-old female C57BL/6 mice were purchased from Charles River Laboratories. $HDC^{-/-}$ (56) and H1R and H2R knockout (H1$R^{-/-}$ and H2$R^{-/-}$) (57, 58) mice were provided by H. Ohtsu and T. Watanabe, respectively. All knockout mice originated from the C57BL/6 background.

The mice, including OT-1 and OT-2 transgenic mice (59), were bred in our animal facility. OT-1 mice are transgenic for a TCR that recognizes the OVA peptide 257–264 in the context of $H2K^b$. OT-2 mice express a

transgenic TCR, which recognizes the OVA peptide 323–339 in the context of I-A^b. All animal care and experimentation were conducted in accordance with the Pasteur Institute animal care and use committee guidelines.

An. stephensi (SDA 500 strain) mosquitoes were raised at the Center of Production and Infection of Anopheles (CEPIA) of the Institut Pasteur using standard procedures, as previously described (1).

Parasites and infection. For all infections, *Pb* NK65 or *Pb* ANKA lines expressing GFP on circumsporozoite (60) or the hsp70 promoter (61), respectively, were used to allow the detection of sporozoites in living mosquitoes. *Pb* ANKA was provided by T. Ishino (Mie University School of Medicine, Edobashi, Tsu, Japan). This parasite induces experimental CM, characterized by paralysis, ataxia, convulsions, and coma between 7–9 d after infection. *Pb* NK65 induces lethal malaria without neurological symptoms and was provided by R. Ménard (Institut Pasteur, Paris, France). These parasites were maintained in a cycle between C57BL/6 mice and *An. stephensi*. The erythrocytic stages of the parasite were maintained in liquid nitrogen as parasitized RBCs (pRBCs) in Alsever's solution (Sigma-Aldrich) containing 10% glycerol. The infection was induced by i.p. injection of 10^6 pRBCs or by exposure of mice to mosquito bites (seven to nine bites per mouse).

Treatment with antihistamine drugs. The histamine receptor subclass-specific inhibitors cimetidine, imetit, and JNJ 7777120 (H2R, H3R, and H4R, respectively; Sigma-Aldrich) were injected i.p. daily at 10 mg/kg for 10 d, starting 24 h before infection. Levocetirizine (H1R), obtained from UCB, was used at 10 mg/kg. Histamineamia was determined using ELISA kits purchased from Neogen Corporation.

Preparation of brain cell suspensions. The brains were obtained from wild-type–susceptible C57BL/6 mice at the coma stage of CM and at the same time from $HDC^{-/-}$ mice (day 6). In brief, mice anesthetized with 600 mg/kg ketamine and 20 mg/kg xylazine were perfused with 150 ml PBS. Each brain was then removed and homogenized in RPMI 1640 medium (BioWhittaker) by passing through sterile meshes to obtain a single-cell suspension. Percoll (GE Healthcare) was added at a final concentration of 35% to the cell pellet and centrifuged at 400 *g* for 20 min at 20°C. The cell pellet was washed twice and analyzed via flow cytometry.

In vivo study of CFSE-labeled T cell proliferation. Splenocytes were prepared from OT-1 and OT-2 mice. Cell suspensions were prepared by passing through sterile meshes. Erythrocytes were lysed using RBC lysis buffer (Sigma-Aldrich). Cells were washed twice in RPMI 1640 medium, and live cells were counted using Trypan blue exclusion staining and adjusted to 10^7 cells per milliliter. $CD8^+$ OT-1 or $CD4^+$ OT-2 cells were purified with MACS beads according to the manufacturer's instructions (Miltenyi Biotec), and cells were stained with allophycocyanin (APC)-conjugated anti-CD8 or APC-conjugated anti-CD4 antibodies, and the purity was ∼95% as evaluated by FACS analysis. Staining of spleen cells with CFSE (Invitrogen) was performed according to the manufacturer's instructions. Recipient mice (C57BL/6, $HDC^{-/-}$) were inoculated 3 d after infection with 10^6 pRBCs i.v. with either 5×10^6 purified CFSE-$CD8^+$ OT-1 or CFSE-$CD4^+$ OT-2 cells. Mice were injected 1 h later with 1 mg OVA. Single-cell suspensions of spleens of the recipients were analyzed 3 d after adoptive cell transfer.

In vivo depletions. Rat IgG2a anti-CD4 mAb (clone GK1.5; American Type Culture Collection) and rat IgG2b anti-CD8 mAb (clone 2.43; American Type Culture Collection) were provided by L. Rénia (Institut Cochin, Paris, France). Purified control rat antibodies were purchased from Sigma-Aldrich. Antibodies were purified from culture supernatants by ammonium sulfate precipitation. Mice were injected i.p. with 500 µg anti-CD8 mAb, anti-CD4 mAb, or control rat IgG on days 1 and 0 before challenge. More than 98% of blood $CD8^+$ or $CD4^+$ T cells were depleted by this procedure, as verified by cytofluorometry (FACScan; BD Biosciences) using anti-CD4 (clone H129-19; Sigma-Aldrich) and anti-CD8 (clone 53-6.7; BD Biosciences) mAbs that recognized epitopes different from those bound by the depleting mAbs. Mice were then injected with 10^6 pRBCs infected with *Pb* ANKA, and 200 µg of antibodies was administered every other day until completion of the experiment.

Flow cytometric analysis of brain and spleen leukocytes. Spleen and brain cells were stained for FACS analysis according to standard protocols in cold PBS containing 2% FCS and 0.01% sodium azide (FACS buffer) with the following antibodies: APC-labeled CD4, APC-labeled anti-CD8α, and PE-labeled antiperforin. RBCs were eliminated using cell lysis buffer, and cells were washed in FACS buffer. After staining with anti-CD4 or anti-CD8α antibodies, cells were washed and resuspended in fixation/permeabilization solution for 20 min at 4°C. Fixed/permeabilized cells were resuspended in Perm/Wash buffer (BD Biosciences) for before flow cytometric analysis. A total of 4×10^4 and 10^5 living cells for brain and spleen, respectively, were analyzed using a four-color flow cytometer (FACSCalibur) with CellQuest Pro software (both from BD Biosciences).

Permeability of the BBB. When mice infected with *Pb* ANKA began showing neurological symptoms, usually at day 6–7 after infection, a 200-µl volume of a 2% (wt/vol) solution of Evans blue in PBS was injected into the mice retro-orbitally. 1 h later, mice were perfused with PBS after anesthesia with 600 mg/kg ketamine and 20 mg/kg xylazine. Each brain was removed and photographed.

Animal perfusion and histological analysis. For the May-Grünwald Giemsa (MGG) staining procedure and immunohistochemical studies, the protocols used to obtain 5-µm-thick brain sections were described previously (62). Detection of blood-stage parasites associated with sequestered erythrocytes in the brain could be visualized either by MGG staining or by fluorescence because of their expression of GFP. Images of randomly selected endplates were collected using an upright microscope (BX61; Olympus) equipped with an oil immersion lens (60×) and a cooled video camera (Retiga 2000R; QImaging) with a color conversion filter. Digitizing was performed with a computer using the image analysis system Image-Pro Plus (Media Cybernetics). Detection of VCAM-1 and ICAM-1 was performed by using specific mAbs (clones 429 and 3E2, respectively), followed by biotin-conjugated goat anti–rat IgG-specific polyclonal antibody (for VCAM-1) and mouse anti–hamster antibody (for ICAM-1). Streptavidin peroxidase and 3-amino-9-ethylcarbazole, as substrates, were added thereafter. All antibodies were obtained from BD Biosciences.

Cytokine and chemokine quantification in the brain and serum. To evaluate shifts of immune mediators in serum, LINCOplex protein arrays were performed on day 5 serum samples from $HDC^{-/-}$ and C57BL/6 mice, according to the standard protocol. Cytokine and chemokine expression in the brain at day 7 was analyzed by real-time RT-PCR. RNA used for these assays was isolated by means of a two-step extraction process. First, brains were surgically removed from mice, in Preparation of brain cell suspensions, and placed immediately in RNAlater (Ambion) at 4°C overnight. After RNAlater infused the samples, it was removed and samples were maintained at −80°C until processing. Brains were thawed in 1 ml of TRIzol and subjected to bead disruption in a polytron three times for 2 min at a setting of 30 cycles per second. Samples were spun at high speed (10,000 *g*) for 3 min to remove debris and lipids. Half of the sample was transferred to a new tube and mixed with 500 µl of TRIzol reagent by vortexing. After this step, RNA extraction proceeded according to the manufacturer's protocol. Precipitated RNA was resuspended in 100 µl of RNase-free water. The second step of this extraction was in accordance with the manufacturer's protocol for RNA cleanup, including steps for the removal of protein and DNA (RNeasy kit; QIAGEN). Samples were eluted with 50 µl of RNase-free water, and quality and quantity were assured by photospectroscopy. Real-time RT-PCR used various primer-probe sets and standard Taqman protocols (Applied Biosystems), as previously described (63).

Statistical analysis. Statistical significance was assessed by the Student's *t* test, except for survival. Significant differences in survival were evaluated by the generation of Kaplan-Meier plots and log-rank analysis. $P < 0.05$ was considered statistically significant.

We thank Dr. T. Ishino and R. Ménard for providing GFP–*Plasmodium berghei* parasite strains. We also thank all of the members of CEPIA, at the Institut Pasteur, for providing us with *Anopheles* mosquitoes, as well as H. Kuhn for assisting us with histological work. We are grateful to L. Rénia for his generous gift of anti-CD4 and anti-CD8 mAbs, to E. Schneider for histamine measurements in brain tissues, and to UCB for providing levocetirizine. We thank R. Ménard and S. Pied for their critical readings of the manuscript before publication.

This work was supported by the Institut Pasteur, Sanofi-aventis, and the Ministry of Research Initiative for Fighting against Parasitic Diseases. W. Beghdadi was supported by the Foundation Mérieux.

The authors have no conflicting financial interests.

Submitted: 25 July 2007
Accepted: 4 January 2008

REFERENCES

1. Demeure, C.E., K. Brahimi, F. Hacini, F. Marchand, R. Peronet, M. Huerre, P. St-Mezard, J.F. Nicolas, P. Brey, G. Delespesse, and S. Mecheri. 2005. *Anopheles* mosquito bites activate cutaneous mast cells leading to a local inflammatory response and lymph node hyperplasia. *J. Immunol.* 174:3932–3940.
2. Depinay, N., F. Hacini, W. Beghdadi, R. Peronet, and S. Mecheri. 2006. Mast cell-dependent down-regulation of antigen-specific immune responses by mosquito bites. *J. Immunol.* 176:4141–4146.
3. Kurtzhals, J.A., C.M. Reimert, E. Tette, S.K. Dunyo, K.A. Koram, B.D. Akanmori, F.K. Nkrumah, and L. Hviid. 1998. Increased eosinophil activity in acute *Plasmodium falciparum* infection–association with cerebral malaria. *Clin. Exp. Immunol.* 112:303–307.
4. Nyakeriga, M.A., M. Troye-Blomberg, S. Bereczky, H. Perlmann, P. Perlmann, and G. ElGhazali. 2003. Immunoglobulin E (IgE) containing complexes induce IL-4 production in human basophils: effect on Th1-Th2 balance in malaria. *Acta Trop.* 86:55–62.
5. Furuta, T., T. Kikuchi, Y. Iwakura, and N. Watanabe. 2006. Protective roles of mast cells and mast cell-derived TNF in murine malaria. *J. Immunol.* 177:3294–3302.
6. Bhattacharya, U., S. Roy, P.K. Kar, B. Sarangi, and S.C. Lahiri. 1988. Histamine & kinin system in experimental malaria. *Indian J. Med. Res.* 88:558–563.
7. Maegraith, B., and A. Fletcher. 1972. The pathogenesis of mammalian malaria. *Adv. Parasitol.* 10:49–75.
8. Srichaikul, T., N. Archararit, T. Siriasawakul, and T. Viriyapanich. 1976. Histamine changes in *Plasmodium falciparum* malaria. *Trans. R. Soc. Trop. Med. Hyg.* 70:36–38.
9. Perlmann, P., H. Perlmann, G. ElGhazali, and M.T. Blomberg. 1999. IgE and tumor necrosis factor in malaria infection. *Immunol. Lett.* 65:29–33.
10. Hill, S.J., C.R. Ganellin, H. Timmerman, J.C. Schwartz, N.P. Shankley, J.M. Young, W. Schunack, R. Levi, and H.L. Haas. 1997. International Union of Pharmacology. XIII. Classification of histamine receptors. *Pharmacol. Rev.* 49:253–278.
11. Hofstra, C.L., P.J. Desai, R.L. Thurmond, and W.P. Fung-Leung. 2003. Histamine H4 receptor mediates chemotaxis and calcium mobilization of mast cells. *J. Pharmacol. Exp. Ther.* 305:1212–1221.
12. Bryce, P.J., C.B. Mathias, K.L. Harrison, T. Watanabe, R.S. Geha, and H.C. Oettgen. 2006. The H1 histamine receptor regulates allergic lung responses. *J. Clin. Invest.* 116:1624–1632.
13. Bury, T.B., J.L. Corhay, and M.F. Radermecker. 1992. Histamine-induced inhibition of neutrophil chemotaxis and T-lymphocyte proliferation in man. *Allergy.* 47:624–629.
14. Elenkov, I.J., E. Webster, D.A. Papanicolaou, T.A. Fleisher, G.P. Chrousos, and R.L. Wilder. 1998. Histamine potently suppresses human IL-12 and stimulates IL-10 production via H2 receptors. *J. Immunol.* 161:2586–2593.
15. Shevach, E.M. 2002. CD4+ CD25+ suppressor T cells: more questions than answers. *Nat. Rev. Immunol.* 2:389–400.
16. Bissonnette, E.Y. 1996. Histamine inhibits tumor necrosis factor alpha release by mast cells through H2 and H3 receptors. *Am. J. Respir. Cell Mol. Biol.* 14:620–626.
17. Idzko, M., A. la Sala, D. Ferrari, E. Panther, Y. Herouy, S. Dichmann, M. Mockenhaupt, F. Di Virgilio, G. Girolomoni, and J. Norgauer. 2002. Expression and function of histamine receptors in human monocyte-derived dendritic cells. *J. Allergy Clin. Immunol.* 109:839–846.
18. Burns, A.R., R.A. Bowden, Y. Abe, D.C. Walker, S.I. Simon, M.L. Entman, and C.W. Smith. 1999. P-selectin mediates neutrophil adhesion to endothelial cell borders. *J. Leukoc. Biol.* 65:299–306.
19. Van de Voorde, J., and I. Leusen. 1983. Role of the endothelium in the vasodilator response of rat thoracic aorta to histamine. *Eur. J. Pharmacol.* 87:113–120.
20. Majno, G., S.M. Shea, and M. Leventhal. 1969. Endothelial contraction induced by histamine-type mediators: an electron microscopic study. *J. Cell Biol.* 42:647–672.
21. Svensjo, E., and G.J. Grega. 1986. Evidence for endothelial cell-mediated regulation of macromolecular permeability by postcapillary venules. *Fed. Proc.* 45:89–95.
22. Enwonwu, C.O., B.M. Afolabi, L.O. Salako, E.O. Idigbe, and N. Bashirelah. 2000. Increased plasma levels of histidine and histamine in falciparum malaria: relevance to severity of infection. *J. Neural Transm.* 107:1273–1287.
23. Belnoue, E., M. Kayibanda, J.C. Deschemin, M. Viguier, M. Mack, W.A. Kuziel, and L. Renia. 2003. CCR5 deficiency decreases susceptibility to experimental cerebral malaria. *Blood.* 101:4253–4259.
24. Medana, I.M., and G.D. Turner. 2006. Human cerebral malaria and the blood-brain barrier. *Int. J. Parasitol.* 36:555–568.
25. Schilling, L., and M. Wahl. 1994. Opening of the blood-brain barrier during cortical superfusion with histamine. *Brain Res.* 653:289–296.
26. Kermode, A.G., A.J. Thompson, P. Tofts, D.G. MacManus, B.E. Kendall, D.P. Kingsley, I.F. Moseley, P. Rudge, and W.I. McDonald. 1990. Breakdown of the blood-brain barrier precedes symptoms and other MRI signs of new lesions in multiple sclerosis. Pathogenetic and clinical implications. *Brain.* 113:1477–1489.
27. Theoharides, T.C. 1990. Mast cells: the immune gate to the brain. *Life Sci.* 46:607–617.
28. Bauer, P.R., H.C. Van Der Heyde, G. Sun, R.D. Specian, and D.N. Granger. 2002. Regulation of endothelial cell adhesion molecule expression in an experimental model of cerebral malaria. *Microcirculation.* 9:463–470.
29. Finley, R.W., L.J. Mackey, and P.H. Lambert. 1982. Virulent *P. berghei* malaria: prolonged survival and decreased cerebral pathology in cell-dependent nude mice. *J. Immunol.* 129:2213–2218.
30. McEver, R.P. 1992. Leukocyte–endothelial cell interactions. *Curr. Opin. Cell Biol.* 4:840–849.
31. Carlos, T.M., and J.M. Harlan. 1994. Leukocyte-endothelial adhesion molecule. *Blood.* 84:2068–2101.
32. Kimura, S., K.Y. Wang, A. Tanimoto, Y. Murata, Y. Nakashima, and Y. Sasaguri. 2004. Acute inflammatory reactions caused by histamine via monocytes/macrophages chronically participate in the initiation and progression of atherosclerosis. *Pathol. Int.* 54:465–474.
33. Ciprandi, G., M.A. Tosca, C. Cosentino, A.M. Riccio, G. Passalacqua, and G.W. Canonica. 2003. Effects of fexofenadine and other antihistamines on components of the allergic response: adhesion molecules. *J. Allergy Clin. Immunol.* 112:S78–S82.
34. de Blic, J., U. Wahn, E. Billard, R. Alt, and M.C. Pujazon. 2005. Levocetirizine in children: evidenced efficacy and safety in a 6-week randomized seasonal allergic rhinitis trial. *Pediatr. Allergy Immunol.* 16:267–275.
35. Alonso, A., S.S. Jick, and M.A. Hernan. 2006. Allergy, histamine 1 receptor blockers, and the risk of multiple sclerosis. *Neurology.* 66:572–575.
36. Lachapelle, J.M., J. Decroix, A. Henrijean, P.P. Roquet-Gravy, A. De Swerdt, H. Boonen, M. Lecuyer, E. Suys, G. Speelman, and N. Vastesaeger. 2006. Desloratadine 5 mg once daily improves the quality of life of patients with chronic idiopathic urticaria. *J. Eur. Acad. Dermatol. Venereol.* 20:288–292.
37. MacDonald, S.M., J. Bhisutthibhan, T.A. Shapiro, S.J. Rogerson, T.E. Taylor, M. Tembo, J.M. Langdon, and S.R. Meshnick. 2001. Immune mimicry in malaria: *Plasmodium falciparum* secretes a functional histamine-releasing factor homolog in vitro and in vivo. *Proc. Natl. Acad. Sci. USA.* 98:10829–10832.
38. Amani, V., A.M. Vigário, E. Belnoue, M. Marussig, L. Fonseca, D. Mazier, and L. Rénia. 2000. Involvement of IFN-gamma receptor-medicated signaling in pathology and anti-malarial immunity induced by *Plasmodium berghei* infection. *Eur. J. Immunol.* 30:1646–1655.

39. Lou, J., Y. Gasche, L. Zheng, B. Critico, C. Monso-Hinard, P. Juillard, P. Morel, W.A. Buurman, and G.E. Grau. 1998. Differential reactivity of brain microvascular endothelial cells to TNF reflects the genetic susceptibility to cerebral malaria. *Eur. J. Immunol.* 28:3989–4000.
40. Kossodo, S., C. Monso, P. Juillard, T. Velu, M. Goldmani, and G.E. Grau. 1997. Interleukin-10 modulates susceptibility in experimental cerebral malaria. *Immunology.* 91:536–540.
41. Baptista, J.L., G. Vanham, M. Wery, and E. Van Marck. 1997. Cytokine levels during mild and cerebral falciparum malaria in children living in a mesoendemic area. *Trop. Med. Int. Health.* 2:673–679.
42. Saeftel, M., A. Krueger, S. Arriens, V. Heussler, P. Racz, B. Fleischer, F. Brombacher, and A. Hoerauf. 2004. Mice deficient in interleukin-4 (IL-4) or IL-4 receptor alpha have higher resistance to sporozoite infection with *Plasmodium berghei* (ANKA) than do naive wild-type mice. *Infect. Immun.* 72:322–331.
43. Edvinsson, L., and B.B. Fredholm. 1983. Characterization of adenosine receptors in isolated cerebral arteries of cat. *Br. J. Pharmacol.* 80:631–637.
44. Wahl, M., and L. Schilling. 1993. Regulation of cerebral blood flow–a brief review. *Acta Neurochir. Suppl. (Wien).* 59:3–10.
45. Newton, C.R., N. Peshu, B. Kendall, F.J. Kirkham, A. Sowunmi, C. Waruiru, I. Mwangi, S.A. Murphy, and K. Marsh. 1994. Brain swelling and ischaemia in Kenyans with cerebral malaria. *Arch. Dis. Child.* 70:281–287.
46. Belnoue, E., M. Kayibanda, A.M. Vigario, J.C. Deschemin, N. van Rooijen, M. Viguier, G. Snounou, and L. Renia. 2002. On the pathogenic role of brain-sequestered alphabeta CD8+ T cells in experimental cerebral malaria. *J. Immunol.* 169:6369–6375.
47. Grau, G.E., P.F. Piguet, H.D. Engers, J.A. Louis, P. Vassalli, and P.H. Lambert. 1986. L3T4+ T lymphocytes play a major role in the pathogenesis of murine cerebral malaria. *J. Immunol.* 137:2348–2354.
48. Yanez, D.M., D.D. Manning, A.J. Cooley, W.P. Weidanz, and H.C. van der Heyde. 1996. Participation of lymphocyte subpopulations in the pathogenesis of experimental murine cerebral malaria. *J. Immunol.* 157:1620–1624.
49. Favre, N., C. Da Laperousaz, B. Ryffel, N.A. Weiss, B.A. Imhof, W. Rudin, R. Lucas, and P.F. Piguet. 1999. Role of ICAM-1 (CD54) in the development of murine cerebral malaria. *Microbes Infect.* 1:961–968.
50. Shimizu, T., J. Nishihira, H. Watanabe, R. Abe, T. Ishibashi, and H. Shimizu. 2004. Cetirizine, an H1-receptor antagonist, suppresses the expression of macrophage migration inhibitory factor: its potential anti-inflammatory action. *Clin. Exp. Allergy.* 34:103–109.
51. Delahaye, N.F., N. Coltel, D. Puthier, L. Flori, R. Houlgatte, F.A. Iraqi, C. Nguyen, G.E. Grau, and P. Rihet. 2006. Gene-expression profiling discriminates between cerebral malaria (CM)-susceptible mice and CM-resistant mice. *J. Infect. Dis.* 193:312–321.
52. Kaul, D.K., X.D. Liu, R.L. Nagel, and H.L. Shear. 1998. Microvascular hemodynamics and in vivo evidence for the role of intercellular adhesion molecule-1 in the sequestration of infected red blood cells in a mouse model of lethal malaria. *Am. J. Trop. Med. Hyg.* 58:240–247.
53. Wilson, N.S., G.M. Behrens, R.J. Lundie, C.M. Smith, J. Waithman, L. Young, S.P. Forehan, A. Mount, R.J. Steptoe, K.D. Shortman, et al. 2006. Systemic activation of dendritic cells by Toll-like receptor ligands or malaria infection impairs cross-presentation and antiviral immunity. *Nat. Immunol.* 7:165–172.
54. Kownatzki, E. 1984. Clearance of histamine from the peritoneal cavity of rats. *Agents Actions.* 15:249–253.
55. Nakornchai, S., and P. Konthiang. 2006. Potentiation of antimalarial drug action by chlorpheniramine against multidrug-resistant *Plasmodium falciparum* in vitro. *Parasitol. Int.* 55:195–199.
56. Ohtsu, H., S. Tanaka, T. Terui, Y. Hori, Y. Makabe-Kobayashi, G. Pejler, E. Tchougounova, L. Hellman, M. Gertsenstein, N. Hirasawa, et al. 2001. Mice lacking histidine decarboxylase exhibit abnormal mast cells. *FEBS Lett.* 502:53–56.
57. Inoue, I., K. Yanai, D. Kitamura, I. Taniuchi, T. Kobayashi, K. Niimura, T. Watanabe, and T. Watanabe. 1996. Impaired locomotor activity and exploratory behavior in mice lacking histamine H1 receptors. *Proc. Natl. Acad. Sci. USA.* 93:13316–13320.
58. Kobayashi, T., S. Tonai, Y. Ishihara, R. Koga, S. Okabe, and T. Watanabe. 2000. Abnormal functional and morphological regulation of the gastric mucosa in histamine H2 receptor-deficient mice. *J. Clin. Invest.* 105: 1741–1749.
59. Hogquist, K.A., S.C. Jameson, W.R. Heath, J.L. Howard, M.J. Bevan, and F.R. Carbone. 1994. T cell receptor antagonist peptides induce positive selection. *Cell.* 76:17–27.
60. Natarajan, R., V. Thathy, M.M. Mota, J.C. Hafalla, R. Menard, and K.D. Vernick. 2001. Fluorescent *Plasmodium berghei* sporozoites and pre-erythrocytic stages: a new tool to study mosquito and mammalian host interactions with malaria parasites. *Cell. Microbiol.* 3:371–379.
61. Ishino, T., Y. Orito, Y. Chinzei, and M. Yuda. 2006. A calcium-dependent protein kinase regulates *Plasmodium* ookinete access to the midgut epithelial cell. *Mol. Microbiol.* 59:1175–1184.
62. Serviere, J., D. Dubayle, and D. Menetrey. 2003. Increase of rat medial habenular mast cell numbers by systemic administration of cyclophosphamide. *Toxicol. Lett.* 145:143–152.
63. Schneider, B.S., L. Soong, N.S. Zeidner, and S. Higgs. 2004. *Aedes aegypti* salivary gland extracts modulate anti-viral and TH1/TH2 cytokine responses to sindbis virus infection. *Viral Immunol.* 17:565–573.